

# Liquid-gas phase transition in finite nuclei

J. N. De<sup>1)</sup>, S. K. Samaddar<sup>2)</sup> and S. Shlomo<sup>3)</sup>

1) *Variable Energy Cyclotron Centre, 1/AF Bidhan Nagar, Calcutta 700 064, India*

2) *Saha Institute of Nuclear Physics, 1/AF Bidhan Nagar, Calcutta 700 064, India*

3) *Cyclotron Institute, Texas A&M University, College Station, TX 77843-3366, USA*

## Abstract

In a finite temperature Thomas-Fermi framework, we calculate density distributions of hot nuclei enclosed in a freeze-out volume of few times the normal nuclear volume and then construct the caloric curve, with and without inclusion of radial collective flow. In both cases, the calculated specific heats  $C_v$  show a peaked structure signalling a liquid-gas phase transition. Without flow, the caloric curve indicates a continuous phase transition whereas with inclusion of flow, the transition is very sharp. In the latter case, the nucleus undergoes a shape change to a bubble from a diffuse sphere at the transition temperature.

## 1. INTRODUCTION

The equation of state (EOS) of nuclear matter constructed with realistic effective interactions [1] shows that the nuclear liquid coexists in phase-equilibrium with the vapour surrounding it below a critical temperature  $\approx 15 - 20$  MeV. Searching for signals for liquid-gas phase transition in nuclear matter or in finite nuclei has become one of the fundamental issues in medium and higher energy nuclear collisions in recent times after the initial experimental observations of a power law behaviour in the mass or charge distribution of nuclear fragments in proton and heavy ion induced reactions which is usually taken to be indicative of a critical behaviour [2]. On the other hand, different models of liquid-gas phase equilibrium in nuclei [1, 3] show that there is a limiting temperature beyond which the nucleus is unstable and the nuclear liquid and the surrounding gas can not coexist in thermodynamic equilibrium. The limitation in temperature also seems to be an experimentally supported observation [4]. A possible connection between the phase transition temperature and the limiting temperature is therefore called for. Normally phase transitions are signalled by peaks in the specific heat  $C_v$  at constant volume as temperature increases. The microcanonical algorithm of Gross [5] designed for multifragmentation calculations show such a peaked structure for  $C_v$ , so also the calculations by the Copenhagen school [6] in a canonical description. Recent calculations by Dasgupta et al. [7] in the lattice gas model for fragmentation also show such a peak for the specific heat. These calculations however do not allow for any detailed study of the changes in the density distribution at criticality.

Renewed interest in the liquid-gas phase transition has been fueled further by the recent experimental observation [8] that in Au+Au collisions at 600A MeV, the temperature in the caloric curve remains almost constant in the excitation energy range of  $\approx 4 - 10$  MeV per nucleon. This is reminiscent of a first order phase transition and the width in the excitation energy at constant temperature may be called the latent heat for liquid-vapour phase transition. Another set of experimental data with Au on C is reported recently [9] at a little higher energy of 1A GeV where the caloric curve looks somewhat different; here around 6-7 MeV the temperature rises slowly but steadily with excitation energy indicative of a continuous phase transition. These two different behaviours in the caloric curve possibly reflect subtle changes in the physical process as the bombarding energy increases or as the colliding mass changes. In this paper, we propose an explanation for them in a finite temperature Thomas-Fermi theory (FTTF). Part of the work has been published recently [10].

## 2. THEORETICAL FRAMEWORK

In the following, we give a brief outline for determining the density profiles of hot nuclei in the FTTF approximation starting from an effective nucleon-nucleon interaction.

### 2.1. The interaction

The energy density of the nucleus is calculated with a Seyler-Blanchard type momentum and density dependent finite range two-body effective interaction [1]. It is given by

$$v_{eff}(r, p, \rho) = C_{l,u}[v_1(r, p) + v_2(r, \rho)] \quad (1)$$

$$v_1 = -(1 - p^2/b^2)f(\vec{r}_1, \vec{r}_2),$$

$$v_2 = d^2[\rho_1(r_1) + \rho_2(r_2)]^n f(\vec{r}_1, \vec{r}_2) \quad (2)$$

with

$$f(\vec{r}_1, \vec{r}_2) = \frac{e^{-|\vec{r}_1 - \vec{r}_2|/a}}{|\vec{r}_1 - \vec{r}_2|/a}. \quad (3)$$

Here  $a$  is the range of the interaction,  $b$  denotes its strength of repulsion in the momentum dependence,  $r = |\vec{r}_1 - \vec{r}_2|$  and  $p = |\vec{p}_1 - \vec{p}_2|$  are the relative distance and momenta of the two interacting nucleons. The subscripts  $l$  and  $u$  in the strength  $C$  refer to like pair (n-n or p-p) or unlike pair (n-p) interaction respectively,  $d$  and  $n$  are measures of the strength of the density dependence of the interaction and  $\rho_1$  and  $\rho_2$  are the densities at the sites of the two nucleons. The values of the potential parameters are given in [11].

### 2.2. Self-consistent density profile and the caloric curve

The interaction energy density for a finite nucleus with the interaction chosen is given by

$$\begin{aligned} \varepsilon_I(r) = \frac{2}{h^3} \sum_{\tau} \left[ \frac{1}{h^3} \int \{v_1(|\vec{r} - \vec{r}'|, |\vec{p} - \vec{p}'|) + v_2(|\vec{r} - \vec{r}'|, \rho)\} \times \right. \\ \left. \{C_l n_{\tau}(\vec{r}', \vec{p}') + C_u n_{-\tau}(\vec{r}', \vec{p}')\} n_{\tau}(\vec{r}, \vec{p}) \right] d\vec{r}' d\vec{p} d\vec{p}', \end{aligned} \quad (4)$$

and the kinetic energy density is given by

$$\mathcal{K}(r) = \frac{2}{h^3} \sum_{\tau} \int \frac{p^2}{2m_{\tau}} n_{\tau}(\vec{r}, \vec{p}) d\vec{p}. \quad (5)$$

Here  $\tau$  is the isospin index,  $n_\tau(\vec{r}, \vec{p})$  the occupation probability and  $m_\tau$  the nucleon mass. The coulomb interaction energy density is taken to be the sum of the direct and exchange term.

The occupation probability is obtained by minimising the thermodynamic potential

$$G = E - TS - \sum_{\tau} \mu_{\tau} A_{\tau}, \quad (6)$$

where E and S are total energy and entropy of the system at temperature T and  $A_{\tau}$  the number of neutrons or protons,  $\mu_{\tau}$  being their chemical potential. In the local density approximation, the occupation probability can be written as

$$n_{\tau}(\vec{r}, \vec{p}) = [1 + \exp\{(\frac{p^2}{2m_{\tau}^*(r)} + V_{\tau}^0(r) + V_{\tau}^2(r) + \delta_{\tau,p}V_c(r) - \mu_{\tau})/T\}]^{-1}, \quad (7)$$

where  $m_{\tau}^*(r)$  is the effective mass dependent on the momentum dependent part of the single particle potential  $p^2V_{\tau}^1(r)$  and  $V_{\tau}^0, V_{\tau}^1, V_{\tau}^2, V_c$  etc are potential terms expressions of which in terms of density are given in Ref.[11]. The density is the momentum integral of the occupancy. The total energy density is then written as

$$\varepsilon(r) = \sum_{\tau} \rho_{\tau}(r)[T J_{3/2}(\eta_{\tau}(r))/J_{1/2}(\eta_{\tau}(r))(1 - m_{\tau}^*(r)V_{\tau}^1(r)) + \frac{1}{2}(V_{\tau}^0 + \delta_{\tau,p}V_c(r))], \quad (8)$$

where  $J_K$  are the Fermi integrals and the fugacity  $\eta_{\tau}(r)$  is defined as

$$\eta_{\tau}(r) = [\mu_{\tau} - V_{\tau}^0(r) - V_{\tau}^2(r) - \delta_{\tau,p}V_c(r)]/T. \quad (9)$$

The total energy per particle  $E(T)$  is obtained from the energy density. The excitation energy per particle is then calculated as  $E^* = E(T) - E(T = 0)$ .

The continuum states of a nucleus at a nonzero temperature are occupied with a finite probability. The particle density therefore does not vanish at large distances. The observables then depend on the size of the box in which the calculations are done. In model calculations in heavy ion collisions, it is usually assumed that thermalisation occurs in a freeze-out volume significantly larger than the normal nuclear volume. Guided by this common practice, we fix a volume, find out the density profiles and obtain the caloric curve, the excitation energy as a function of temperature. The specific heat at constant volume is then calculated as  $C_v = (dE^*/dT)_v$ .

Starting from the guess density, one can arrive at a self-consistent density iteratively and calculate the physical observables. The details are given in [11].

### 2.3. Inclusion of collective radial flow

A hot nuclear system created in the laboratory from energetic nuclear collisions may be initially compressed. In the decompression phase, a collective radial flow may be generated in addition to thermal excitation. An expanding system, in a strict thermodynamic sense is not in equilibrium. However, if the time scale involved in the expansion is much larger compared to the equilibration times in the expanding complex, the thermodynamic equilibrium concept may still be meaningful. In a recent paper, Pal et al. [12] suggested that the effect of collective radial flow could be simulated through the inclusion of an external negative pressure in the total thermodynamic potential at freeze-out volume. A positive uniform external pressure gives rise to compression; similarly a negative pressure gives rise to an inflationary scenario resulting in the outward radial flow of matter. The expanding system can hence be assumed to be under the action of a negative external pressure  $P_0$ . Its magnitude is equal to flow pressure  $P_f$  ( $|P_0| = P_f$ ), the internal

pressure exerted by the radially outgoing nucleons at the freezeout surface. The total thermodynamic potential of the system at freezeout then is given by

$$G = E - TS - \sum_{\tau} \mu_{\tau} A_{\tau} + P_0 \Omega, \quad (10)$$

where  $P_0$  is the constant external pressure assumed negative and  $\Omega$  the effective volume. It is given as

$$\Omega = \frac{4}{3}\pi R^3, \quad R = \left(\frac{5}{3} \langle r^2 \rangle\right)^{1/2}. \quad (11)$$

Here  $\langle r^2 \rangle^{1/2}$  is the rms radius of the matter density distribution and  $R$  is the radius of the corresponding uniform density distribution. The occupancy obtained from the minimisation of the thermodynamic potential then contains a pressure term and reads as

$$n_{\tau}(\vec{r}, \vec{p}) = [1 + \exp\left\{\left(\frac{p^2}{2m_{\tau}^*(r)} + V_{\tau}^0(r) + V_{\tau}^2(r) + \delta_{\tau p} V_c(r) - \mu_{\tau} + P_0 \frac{10\pi}{3A} Rr^2\right)/T\right\}]^{-1}. \quad (12)$$

With the inclusion of flow, the whole set of calculations can then be repeated with an effective chemical potential

$$\mu_{\tau}^{eff} = \mu_{\tau} - P_0 \frac{10\pi}{3A} Rr^2. \quad (13)$$

It has been shown [12] that the flow pressure  $P_f (= -P_0)$  is related to the flow energy as

$$P_f = D(v_f, T) \rho(r) e_f(r), \quad (14)$$

where the quantity  $D(v_f, T)$  depends weakly on the temperature  $T$  and the radially directed flow velocity  $v_f$  and is  $\simeq 4.5$  for nucleons and  $e_f(r)$  the flow energy per nucleon at any point within the volume. The total flow energy may be expressed as

$$E_f = \int_v \rho(r) e_f(r) d\vec{r} = P_f V / D(v_f, T). \quad (15)$$

Here  $\int_v = V$  is the size of the box or the freeze-out volume in which the calculations are done.

### 3. RESULTS AND DISCUSSIONS

To do calculations in the mass range of experimental interest, we choose two systems, namely,  $^{150}\text{Sm}$  and  $^{85}\text{Kr}$ . We report calculations done in a freeze-out volume  $V = 8V_0$  where  $V_0$  is the normal volume of the nucleus at zero temperature. The freeze-out volume chosen here is consistent with most multifragmentation calculations [5] and we have found that our results are nearly insensitive to volumes much beyond these chosen confinement volumes. Initially, we report calculations without any flow effects. In Figure 1, the proton density for  $^{150}\text{Sm}$  is displayed at four temperatures,  $T = 5$  MeV (long-dashed curve),  $T = 9$  MeV (dotted curve),  $T = 9.5$  MeV (dash curve) and  $T = 10$  MeV (full curve). With increasing temperature, the central density is progressively depleted with thickening of the long tail spread at the boundary. Beyond  $T = 9.5$  MeV, the density change is rather abrupt and at  $T$  close to 10 MeV, the whole system looks like a uniform distribution of matter inside the volume. This is shown by a representative density distribution at  $T = 10$  MeV. The slight bump at the edge of the density is due to the Coulomb force. The caloric curve for the system  $^{150}\text{Sm}$  is shown in Figure 2 (dotted line). Initially the temperature rises faster with excitation energy, then the rise is slower. A kink is observed at  $T \approx 10$  MeV, beyond which the excitation energy rises linearly with temperature. The

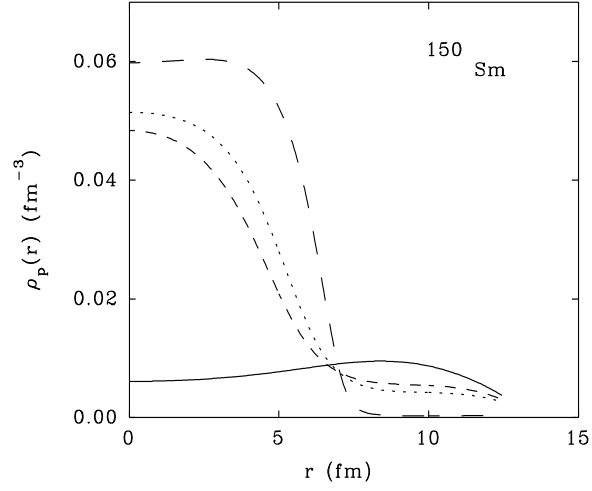


Figure 1: The proton density profile for the system  $^{150}\text{Sm}$  calculated at four temperatures as mentioned in the text.

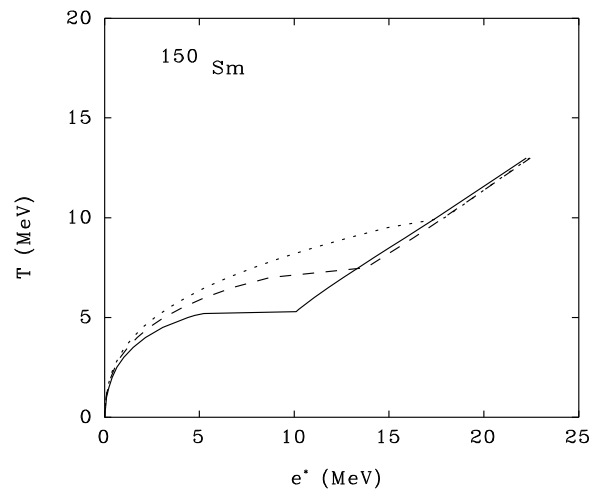


Figure 2: The caloric curve for the system  $^{150}\text{Sm}$  at three pressures.

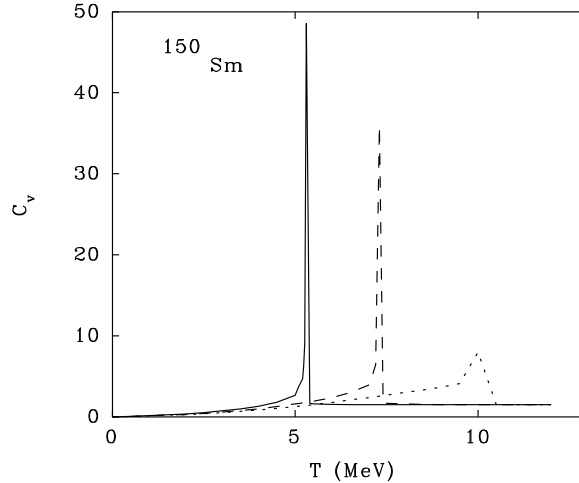


Figure 3: The specific heat per particle plotted as a function of temperature for  $^{150}\text{Sm}$ . The three curves refer to  $P_0 = 0.0$  (dotted),  $P_0 = -0.05$  (dashed) and  $P_0 = -0.1$  (full curve) respectively.

slope  $C_v$  is then  $3/2$  which is a reflection of the fact that the nucleons then behave almost like a classical gas of particles. In Figure 3, the specific heat at constant volume  $C_v$  is displayed (dotted line). It shows a sharp peak at a temperature  $T \simeq 10$  MeV. We believe this to be possibly a signal of the liquid-gas phase transition. The abrupt transition in the density at this temperature and the sharp fall of  $C_v$  to the classical value of  $3/2$  lend credence to our surmise. Collisions between heavy nuclei at high energies may generate a modest amount of compression even for far-central impacts. We have therefore repeated the calculations taking into account the effect of flow energy with different values of  $P_0$ . If  $P_0$  is given, an estimate of the flow energy per nucleon can be easily made with the help of Equations (14) and (15). For example, if  $P_0 = -0.1$  MeV  $fm^{-3}$ , the average flow energy per nucleon is  $\simeq 1.3$  MeV. The caloric curves for  $P_0 = -0.05$  (dashed line) and  $-0.1$  MeV  $fm^{-3}$  (full line) are displayed also in Figure 2. We find that with increase in flow energy, the rise in temperature is slower and when the pressure  $P_0 = -0.1$  MeV  $fm^{-3}$ , the caloric curve shows a plateau at  $T \simeq 5$  MeV in the excitation energy range of 5-10 MeV. In Figure 3, the corresponding specific heats are displayed. The broad-based peak for no flow goes over to an extremely sharp peak from  $T \simeq 10$  MeV to  $T \simeq 5$  MeV with increasing flow. Looking at Figures 2 and 3, it is evident that the system signals a liquid-gas phase transition at the peak temperatures and that the system moves from a continuous phase transition to a sharp first order phase transition. With increase in temperature, it is natural to expect that the rms radius of the nucleus in question would increase. That is displayed in Figure 4. Interestingly, we find that for cases accompanied with flow energy, there is an extremely sharp increase in the rms radius at the phase transition temperature. From Figure 5, we notice that near the phase transition temperature, within an interval of  $\Delta T \approx 0.1$  MeV, the density distribution now undergoes an exotic shape transition to a bubble shape at  $T = 5.3$  MeV. This may be attributed to the loss of surface tension at the transition temperature; when there is flow, the flow pressure pushes the matter outwards which takes a bubble shape because of the constraint of a spherical freeze-out volume. The calculations have been repeated for  $^{85}\text{Kr}$  with freeze-out volume 8 times its normal volume and all the features reported for  $^{150}\text{Sm}$  are reproduced except for the fact that the transition temperature is shifted up by  $\approx 0.5$  MeV and the peak for the specific heat is broader.

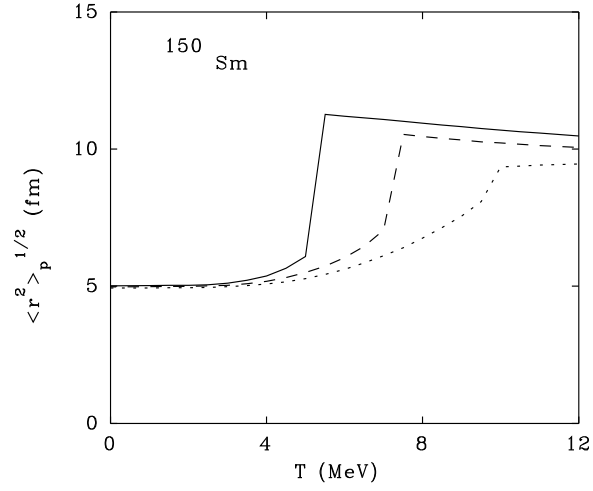


Figure 4: The proton rms radius as a function of temperature for  $^{150}\text{Sm}$  at three pressures.

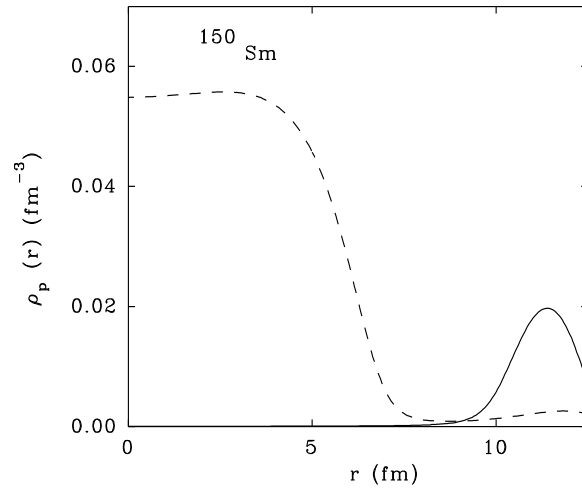


Figure 5: The proton density profile for  $^{150}\text{Sm}$  with  $P_0 = -0.1 \text{ MeV fm}^{-3}$  for  $T = 5.2$  MeV (dashed line) and  $T = 5.3$  (full line) MeV.

## 4. CONCLUSIONS

We have calculated the caloric curve and the specific heat of finite nuclei in a self-consistent finite temperature Thomas-Fermi theory with a realistic effective nucleon-nucleon interaction. The effects of collective radial flow, if any, are built in the theoretical framework. From the caloric curve and the specific heat, signals of liquid-gas phase transition are obtained for cases both with and without collective flow. In the case without flow, there appears to be a continuous phase transition at a temperature  $T \simeq 9.5$  MeV whereas with inclusion of a little flow energy, the phase transition seems to be of first order at a temperature  $T \simeq 5.0$  MeV. The nucleus also then changes its shape from a diffuse sphere to a bubble. A qualitative reference to the two sets of experimental data referred to in the introduction may not be out of place. In the Au induced reaction on C at 1 AGeV, for near peripheral collisions, there is possibly little or no compression because of the small target size. The caloric curve then alludes to a continuous phase transition as theoretically obtained and experimentally reported. For the Au on Au reaction at 600 AMeV, a modest compression and hence radial flow may not be ignored and then a sharper phase transition may result as indicated in the experiments.

This work is partially supported by the U.S. National Science Foundation under grant no. PHY-9413872.

## References

- [1] D. Bandyopadhyay, C. Samanta, S. K. Samaddar and J. N. De, Nucl. Phys. A**511** (1990)1 and references therein.
- [2] M. E. Fisher, Physics **3** (1967)255.
- [3] S. Levit and P. Bonche, Nucl. phys.A **437** (1985) 426.
- [4] J. B. Natowitz et al, in Heavy Ion Dynamics and Hot Nuclei, ed. G. Nebbia and M.N. Namboodiri,(World Scientific,1995) p.1.
- [5] D. H. E. Gross, Rep. prog. phys. **53** (1990)605.
- [6] J. P. Bondorf et al, Phys. Rep. **257** (1995)130.
- [7] S. Dasgupta, J. Pan, I. Kravsnikova and C. Gale, to be published.
- [8] J. Pochodzalla et al, Phys. Rev. Lett. **75** (1995)1040.
- [9] J. A. Hauger et al. Phys. Rev. Lett. **77** (1996)235.
- [10] J. N. De, S. Dasgupta, S. Shlomo and S. K. Samaddar, Phys. Rev. C**55** (1997)R1641.
- [11] J. N. De, N. Rudra, Subrata Pal and S. K. Samaddar, Phys. Rev. C **53** (1996)1.
- [12] S. Pal, S. K. Samaddar and J. N. De, Nucl. Phys.A **608** (1996)49.